Nexo Revista Científica
Vol. 36, No. 06, pp. 1076-1086/Diciembre 2023

ISSN-E 1995-9516
Universidad Nacional de Ingeniería

http://revistas.uni.edu.ni/index.php/Nexo
https://doi.org/10.5377/nexo.v36i06.17465

Morphological and structural properties of bismuth-nickel ferrite synthesized by a combined sol-gel method

Propiedades morfológicas y estructurales de la ferrita de bismuto-níquel sintetizada mediante un método combinado de sol-gel

Ahmed G. Awni*, Zena M. Ali Abbas

Department of Physics, College of Science, University of Diyala, Diyala, Iraq.
*ahmed.ghanim.1995@gmail.com

(recibido/received: 17-agosto-2023; aceptado/accepted: 15-noviembre-2023)

ABSTRACT

In this paper, $Bi_x Ni_{1-x} Fe_2O_4$, (x = 0, 0.3, and 0.5), nanoparticles were synthesized by a sol–gel method, and the synthesized samples were calcination at 350 and 650º C for 3 h. The influence of Bi doping on morphological and structural properties was studied. The field emission scanning electron microscopy (FESEM) analysis showed all of the specimens contain a compact order of homogenous nanoparticles with a spherical form and polyhedral particles with an average size ranging from 36.305 nm to 27.554 nm at 350 and 650º C respectively. By studying the energy dispersive spectrometer analysis patterns, the existence of constituent elements, Ni, Bi, Fe, and O, was verified with a proportion very close to the stoichiometry of the chemical formula. The formation of a ferrite phase was confirmed by X-ray diffraction. An increase in the average crystallite and grain size has been observed with an increase in Bi doping. The Fourier Transform Infrared(FT-IR) studies were made in the frequency range 400-4000 cm^{-1} and observed two strong absorption peaks. The frequency band is found at 555 cm^{-1} whereas the lower frequency band is at 1338.5 cm^{-1}. It is noticed that the two prominent absorption bands were slightly shifted towards the higher frequency side with the increase of Bi3+ ion concentration.

Keywords: Bi-Ni Nanoferrites, Sol-Gel, FESEM, EDS, XRD, FTIR.

RESUMEN

En este artículo, se sintetizaron nanopartículas de Bi x Ni1-x Fe2O4 (x = 0, 0.3 y 0.5) mediante el método sol-gel, y las muestras sintetizadas se calcinaron a 350 y 650 °C durante 3 horas. Se estudió la influencia de la dopación de Bi en las propiedades morfológicas y estructurales. El análisis de microscopía electrónica de barrido de emisión de campo (FESEM) mostró que todas las muestras contenían nanopartículas homogéneas de forma esférica y partículas poliédricas con un tamaño promedio que variaba de 36.305 nm a 27.554 nm a 350 y 650 °C, respectivamente. Mediante el estudio de los patrones de análisis del espectrómetro de dispersión de energía, se verificó la existencia de los elementos constituyentes, Ni, Bi, Fe y O, con una proporción muy cercana a la estequiometría de la fórmula química. La formación de una fase de ferrita se confirmó mediante difracción de rayos X. Se observó un aumento en el tamaño promedio de los cristalitos y en el tamaño de grano con un aumento en la dopación de Bi. Se realizaron estudios de espectroscopía infrarroja por transformada de Fourier (FT-IR) en el rango de frecuencia de 400 a 4000 cm-1 y se observaron

dos picos de absorción fuertes. La banda de frecuencia se encuentra en 555 cm-1, mientras que la banda de frecuencia más baja se encuentra en 1338.5 cm-1. Se observó que los dos picos de absorción prominentes se desplazaron ligeramente hacia el lado de mayor frecuencia con el aumento de la concentración de iones Bi3+.
Palabras claves: Nanoferritas de Bi-Ni, Sol-Gel, FESEM, EDS, XRD, FTIR

1. INTRODUCTION

Spinel-type MFe_2O_4 (where M is a divalent cation) ferrites are a crucial class of magnetic ceramics [Isfahania et al, 2013]. They find applications in electronics ranging from the simplest to the most complicated. Magnetic cards, magnetic media, recording devices, and telecommunications apparatus are just a few of the fascinating places you'll find this material put to use, It is well known that the electrical and magnetic characteristics of spinel ferrites vary depending on factors like their processing conditions and chemical makeup [Nasr Isfahani et al, 2009- Eghbali Arani et al, 2010]. As a soft magnetic n-type semiconducting material [epela´ k et al, 2007- epela´ k et al, 2004], nickel ferrite ($NiFe_2O_4$) is an essential member of the spinel family. A value of 1 for l describes the completely inverse structure of bulk nickel ferrite, It has been discovered that a decrease in particle size and a temperature rise both initiate cation redistribution in a spinel that tends toward a random arrangement [Goldman ,2006- Saeed et al, 2018]. Both the undoped and the substituted versions of $NiFe_2O_4$ are suitable for high-frequency applications in the area of telecommunications. Due to its high resistivity and low eddy current losses, it is used in RF circuits, high-quality filters, rod antennas, transformer cores, read/write heads for high-speed digital tape, and operating devices [Chen et al, 2001 - Saeed et al, 2023].

2. EXPERIMENTAL

2.1 Sample preparation

$Bi_xNi_{(1-x)}Fe_2O_4$ where (x = 0, 0.3, and 0.5) powders were prepared (sol-gel), Starting materials were bismuth nitrate, nickel nitrate, and ferric nitrate. Each of the previously described chemicals was weighed according to the equilibrium ratio and dissolved in (20mL) of deionized water (DW) with continuous stirring at 70 °C. After verifying that there were no sediments or precipitates, some citric acid (14g) dissolved in (50mL) of deionized water (DW) was added, and the solution was thoroughly mixed for (1-2) hours. The complex aqueous solutions were mixed and kept at about 70° C for (1–2) days with vigorous stirring to form a viscous gel solution. The gel was dried at (120° C), which was then collected and pulverized in an agate mortar by grinding. The resultant powders were decomposed at 130 °C in an oven to remove the organic solvents. The obtained aqueous powder was sintered at 350° C and 650°C for (3 hrs). Figure (1) the diagram of sol-gel auto combustion synthesis of $Bi_xNi(1-x)Fe_2O_4$ nanoparticles. More details are in Table (1).

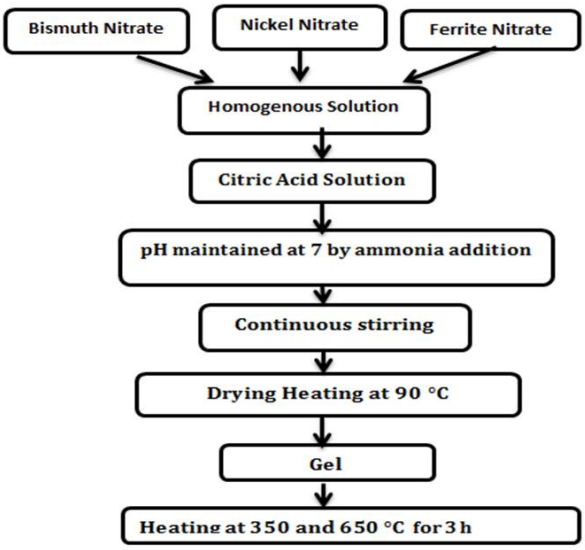

Figure 1. The diagram of the sol-gel synthesis of $Bi_x Ni_{(1-x)} Fe_2 O_4$ nanoparticles.

Table 1. Details of the symbols used.

Sample Name	Material	Heat treatment Temperature (^oC)
B1	$Ni\ Fe_2 O_4$	350^OC
B2	$Bi_{0.3}Ni_{0.7}\ Fe_2 O_4$	350^OC
B3	$Bi_{0.5}\ Ni_{0.5}\ Fe_2 O_4$	350^OC
B4	$Ni\ Fe_2 O_4$	650^OC
B5	$Bi_{0.3}\ Ni_{0.7}\ Fe_2 O_4$	650^OC
B6	$Bi_{0.5}Ni_{0.5}\ Fe_2 O_4$	650^OC

2.2 Characterization

The morphological characteristics of $Bi_x Ni_{(1-x)} Fe_2 O_4$ nanoparticles have been studied by field emission scanning electron microscope (FESEM) and model (ZEISS SIGMAVP/Germany). The structural characteristics of $Bix\ Ni_{(1-x)} Fe_2 O_4$ nanoparticles have been studied by the XRD type (Panalytical X' Pert Pr, UK) and FTIR type (IR Affinty-1CE (FTIR) spectrophotometer).

3. RESULTS AND DISCUSSION

3.1 FE-SEM Analysis

Field emission scanning electron microscopy was used to examine the sample shapes. (FE-SEM). FESEM pictures of bismuth substitution in nickel ferrite samples are shown in Figure (2). It was discovered that the

surface of the images looked rough rather than smooth. The compact sample showed that the grain size distribution was heterogeneous. The surface morphology of the synthesized material revealed that the shape was roughly uniform in micron size as determined by the line intercepts technique[Al-Mgrs et al, 2023], Furthermore, it was discovered that as the nickel substitution in bismuth ferrite increases, the grain size diminishes. The FESEM images demonstrate that the particles have a nearly homogeneous distribution and that some of them are agglomerated. FESEM pictures show that particle aggregation occurs in the nanometer range. During sintering, the pores between the particles were removed, resulting in the creation of strong bonds in the agglomeration form [Aung et al, 2020- Abdullah et al, 2017]. The interaction of grain boundary and porosity is essential in determining the particle's limited grain size. With this research, it was discovered that the average grain size of the particles decreased with Bi+3 ion doping. Table (2) displays the particle size (nm) results of Bi-doped NiFe2 O4 samples.

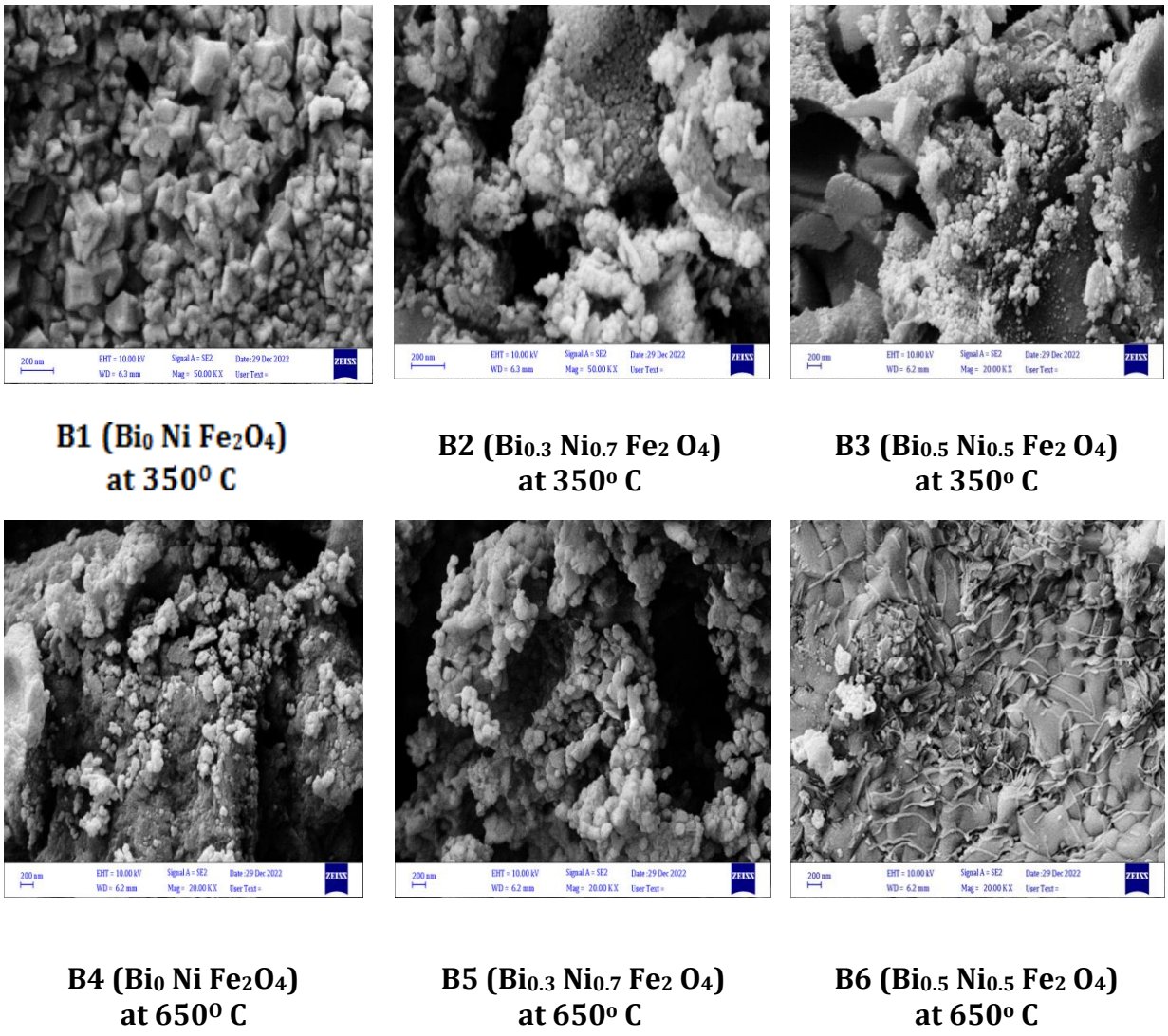

Figure 2. The FE-SEM image of Bi-doped $NiFe_2$ O_4 samples.

Table 2. The particle size (nm) values of Bi-doped $NiFe_2O_4$ samples.

Sample Name	Particle Size (nm)
B1	36.305
B2	31.471
B3	25..173
B4	27.554
B5	22.033
B6	23.132

3.2 EDS Analysis

The EDS analysis has been carried out to examine the chemical composition of the as-obtained samples. Figures (3,4) present the EDS spectra of the samples with B1, B2, B3, B4, B5, and B6, in which peaks of Ni, Bi, Fe, and O elements are detected, and no other impurities can be observed. According to EDS analysis, as the content of (x) increases, the Ni element increases from 38.8 to 42.6 percent at 350 °C and 650°C respectively, As the concentration of (x) increases x=0.3, the nickel element increases from 14.4 to 15.5, while Bismuth element decreases from 44.1 to 41.3 at 350 °C and 650°C respectively, and x=0.5 the nickel element increases from 10.4 to 10.1 while Bismuth element decreases from 57.8 to 53.6 at 350 °C and 650° C respectively. It is noted that the measured elemental ratios of compositions are in agreement with the stoichiometric formula. According to the EDS spectra, with the increase of Bi-doped, the peak intensity of Bismuth increased, whereas the peak intensity for iron and nickel decreased. From the EDS spectra, it is clear that no additional impurities are present in the prepared samples. The peaks of substitution samples imply that bismuth ions enter the ferrite structure [Balideh et al ,2021- Zhou et al, 2004].

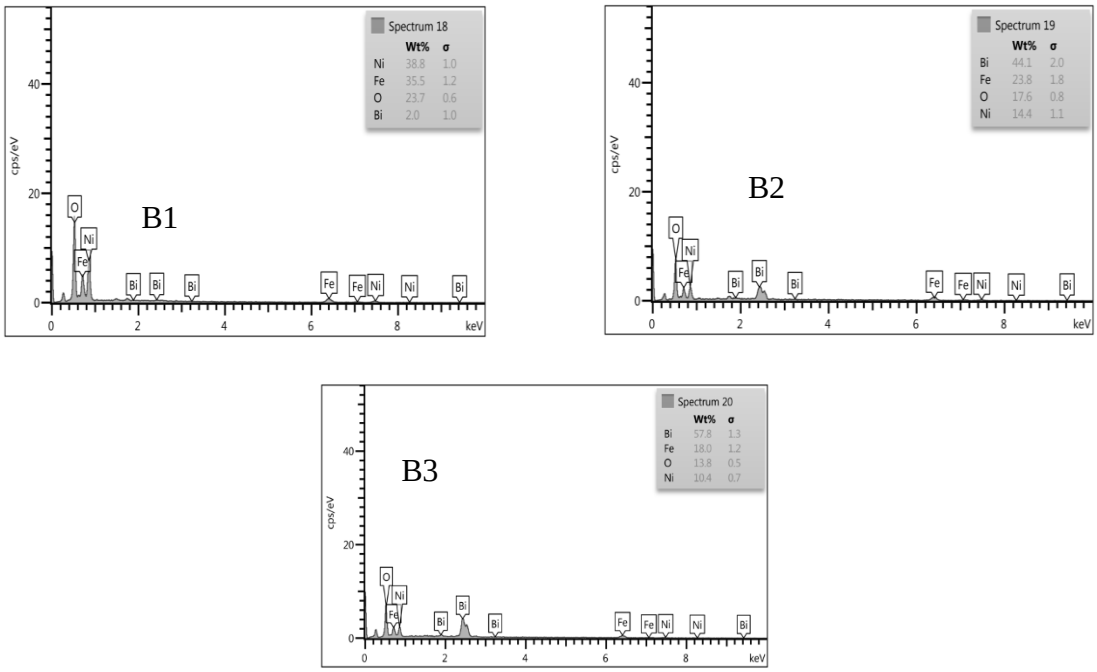

Figure 3. EDS spectra of Bi_x Ni1-x Fe2 O4 nanoferrites for samples at 350oC.

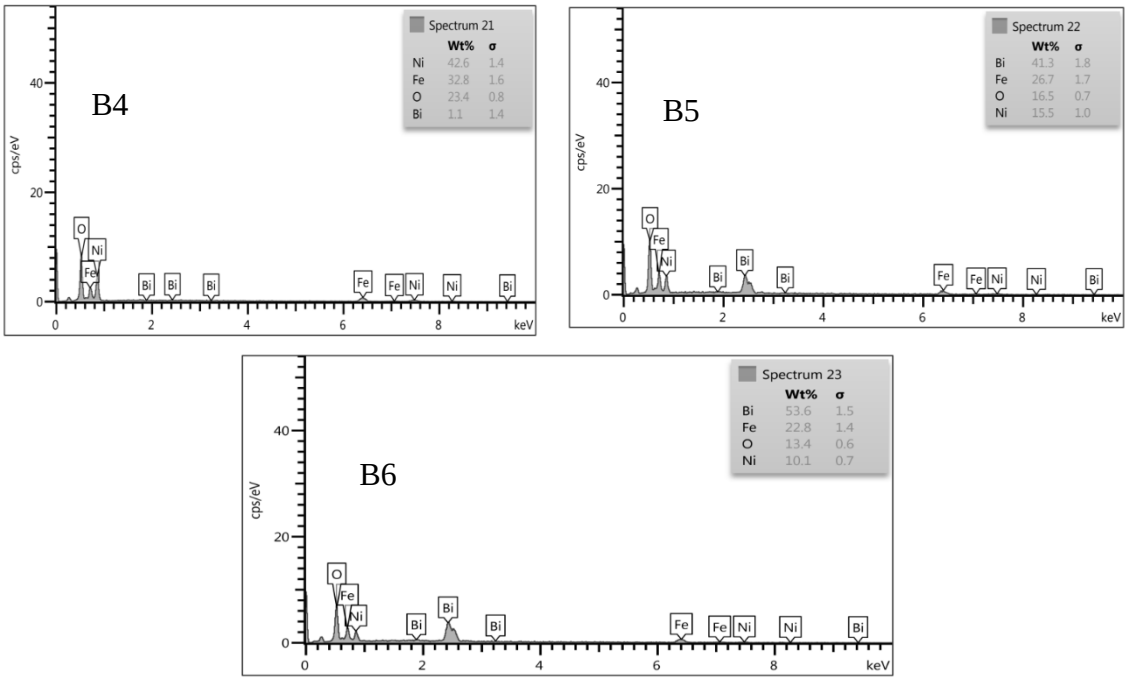

Figure 4. EDS spectra of $Bi_x Ni_{1-x} Fe_2 O_4$ nanoferrites for samples at 650°C.

3.3 X-Ray Diffraction Analysis

The use of the sol-gel method process to synthesize homogeneous and ultrafine nickel ferrites with narrow size distribution at a relatively low calcination temperature, to investigate the effects of calcination temperature and molar ratio on phase composition and morphology of obtained powders. The XRD analysis was performed to study the crystal structure type and crystalline size of prepared Bi x Ni1-x Fe2 O4 ferrite (x= 0, 0.3, and 0.5) at various calcination temperatures (350 and 650 oC). Figures (5,6) show XRD patterns of pure NiFe2O4 ferrite doped with various concentrations of Bi metal (x= 0, 0.3, and 0.5). Figures (5,6) the result show that pure cubic NiFe2 O4 crystal structure with space group (Fd3m), crystal dimensions (a = b = c = 8.339 °A), and crystal angles ($\alpha = \beta = \gamma = 90°$), corresponding with the cubic structure (JCPDS 00-010-0325). The observed peaks at 30.25, 35.69, 37.26, 43.32, 53.91, 57.27, and 62.95 can be assigned to the reflections of (220), (311), (222), (400), (511), and (440) crystal planes, respectively. The presence of intense and sharp peaks revealed that the goods were well-crystallized. Furthermore, it appears that doping with Bi ions has no discernible impact on the crystal structure of NiFe2 O4. No impure phases corresponding to Bi compounds were identified in Bi-doped samples (x= 0, 0.3, and 0.5), indicating that the Bi ions were successfully incorporated into the NiFe2 O4 crystal lattice to form a stable Bi x Ni1-x Fe2 O4 substitution solid solution. More details are in Table (3).

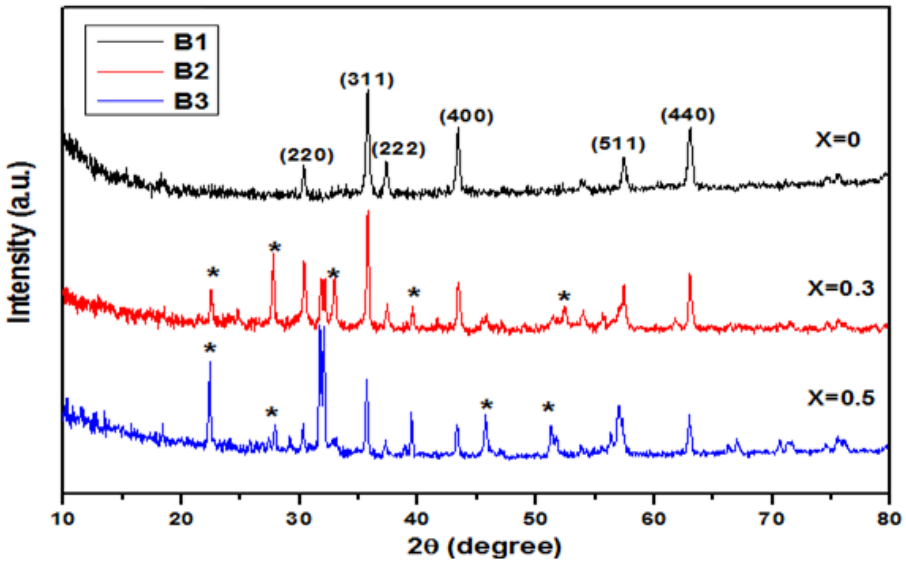

Figure 5. The XRD pattern of $Bi_x Ni_{1-x}Fe_2O_4$ (x = 0, 0.3 and o.5) nano ferrite particles at 350 °C.

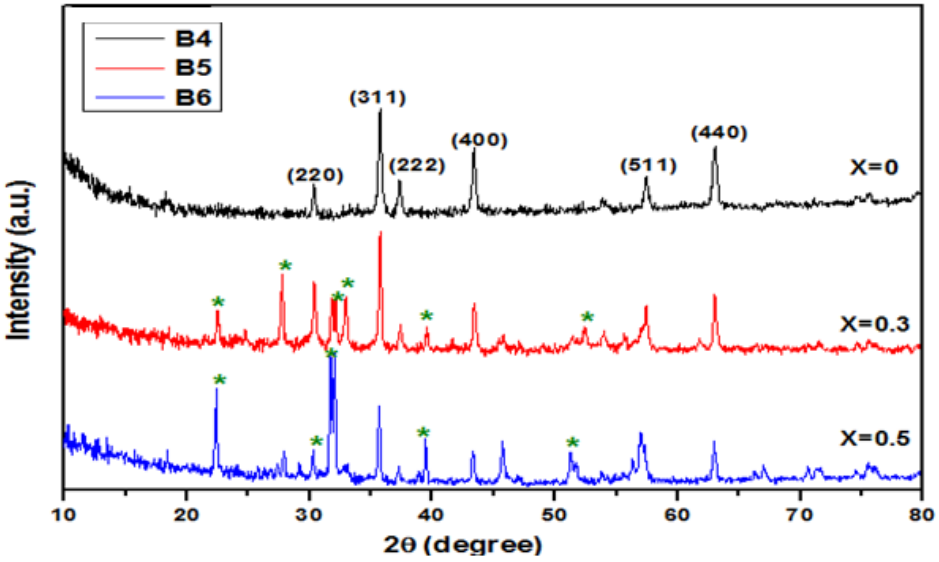

Figure 6. The XRD pattern of $Bi_x Ni_{1-x}Fe_2O_4$ (x = 0, 0.3 and o.5) nanoferrite particles at 650°C.

Table 3. XRD calculations of Bix Ni1-x Fe2 O4 (x=0, 0.3, and 0.5) at different calcination temperatures.

Material	2Θ (deg) Practical	2Θ (deg) Standard	FWHM (deg)	Crystalline size (nm)	d hkl (°A) Practical	d_{hkl} (°A) Standard	(h kl)
B1	30.25	30.29	0.3397	24.23	2.95166	2.94800	(220)
B2	30.29		0.586301	13.55	2.94748		
B3	30.22		0.494688	16.64	2.95461		
B4	30.34		0.291892	28.21	2.94304		
B5	30.37		0.295793	27.84	2.94022		
B6	30.27		0.266883	30.85	2.94947		

B1	35.69	35.7	0.4524	18.45	2.51311	2.51300	(311)
B2	35.7		0.47658	17.52	2.51289		
B3	35.49		0.581603	14.3	2.52670		
B4	35.73		0.258401	32.317	2.51074		
B5	35.75		0.225530	37.02	2.50959		
B6	35.65		0.177962	46.91	2.51590		
B1	37.26	37.31	0.3251	25.8	2.41075	2.40800	(222)
B2	37.33		0.472956	17.73	2.40681		
B3	37.22		0.6218	13.48	2.40066		
B4	37.30		0.223869	37.47	2.40829		
B5	37.39		0.295516	26.89	2.40298		
B6	37.24		0.250982	31.66	2.41240		
B1	43.32	43.36	0.6392	13.37	2.08653	2.08500	(400)
B2	43.32		0.746585	11.45	2.08693		
B3	43.27		0.323678	26.41	2.08905		
B4	43.37		0.267242	32	2.08465		
B5	43.37		0.179088	47.76	2.08636		
B6	43.27		0.129303	66.12	2.08906		
B1	57.27	57.35	0.485095	18.67	1.60723	1.60510	(511)
B2	57.1		0.969708	9.33	1.61167		
B3	56.91		0.694275	13.02	1.61665		
B4	57.40		0.340276	26.62	1.60403		
B5	57.40		0.196744	46.05	1.60390		
B6	57.12		0.105091	86.1	1.61106		
B1	62.95	62.91	0.742739	12.54	1.47531	1.47600	(440)
B2	63		0.714739	13.04	1.47400		
B3	62.91		0.988653	9.42	1.47606		
B4	62.99		0.315000	29.59	1.47447		
B5	63.04		0.283546	32.7	1.47336		
B6	62.96		0.197638	47.15	1.47492		

3.4 FT-IR Analysis

Figures (7, 8) show the FTIR spectra of B_x Ni $_{1-x}Fe_2$ O_4 (x =0, 0.3, and 0.5) nano ferrite samples recorded in the 400-4000 cm^{-1} region. It has been reported that the IR bands of solids are typically assigned to the vibration of ions in the crystal lattice [Saeed et al, 2017- Zaki et al, 2010].

The FTIR characterization of a pure Ni Fe_2 O_4 sample synthesized at 350 and 650 C was done to observe the stretching and bending behavior of various oxides. The spectra of the synthesized sample showed the clear existence of peaks at 555 cm-1 which confirms the existence of Ni-O and Fe-O stretching and bending vibrations. The stretching and bending vibrations for Ni-O and Fe-O are almost the same, which gives the idea of the formation of the ferrite phase [Kambale et al, 2011- Srivastava et al, 2009]. Peaks near 845cm^{-1} and 1338.5cm^{-1} represent the presence of nitrate ions, and 2349.2cm^{-1} is the representation of a nitrile It is clear that as the temperature increases, the peaks of nitrate ions become more pronounced, which is in agreement with the FTIR spectra of pure NFO samples. Furthermore, as compared to pure NFO samples, all the peaks present in the FTIR spectra of Bi-doped NFO have shifted a little to a different value. The differences in band positions will be calculated due to the difference in bond length of Fe^{+3} and O_2 ions at the octahedral and tetrahedral sites [Maensiri et al,2007]. Because tetrahedral dimensions are smaller than

octahedral site dimensions, the absorption bands have an inverse association with bond length. It was also discovered that as bismuth content increased, bands v1 and v2 moved slightly to the higher frequency side. Because of the reduction in site radius, the fundamental frequency and thus the central frequency should shift to the higher frequency side [Abdullah et al ,2019- Srivastava et al, 2010].

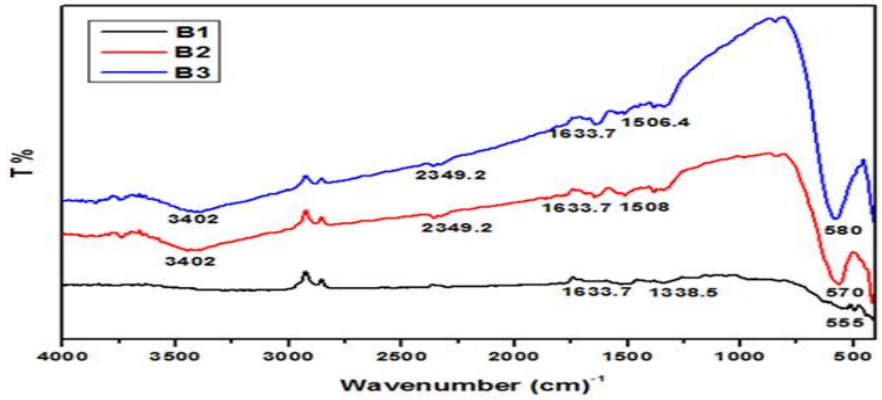

Figure 7. FTIR of Bi-Ni ferrite nanoparticles which are sintered at 350˚C of the composition Bix Ni1-xFe2O4 (x = 0, 0.3, and 0.5).

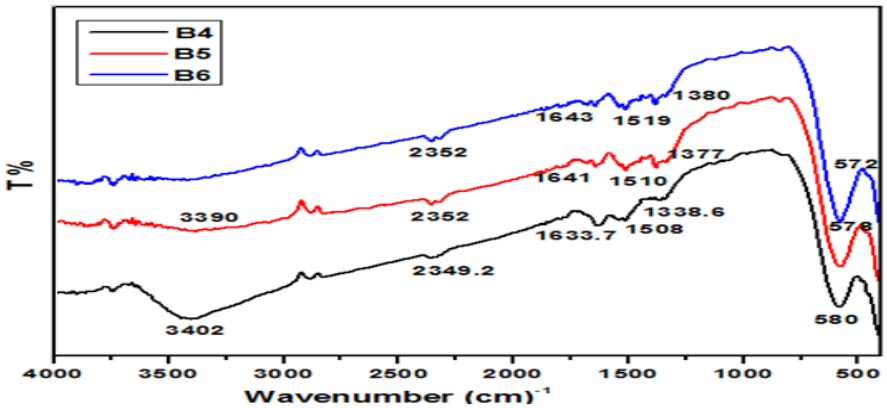

Figure 8. FTIR of Bi-Ni ferrite nanoparticles which are sintered at 650˚C of the composition Bix Ni1-xFe2O4 (x = 0, 0.3, and 0.5).

4. CONCLUSIONS

In summary, the nickel-bismuth nanoparticles were synthesized using the stoichiometric formula Bix Ni1-x Fe2 O4, (x = 0, 0.3, and 0.5), respectively), successfully using the Sol-Gel spontaneous combustion process where the burnt and sintered samples at 350 °C and 650 oC. It is observed that the sol-gel combustion method is a convenient way for obtaining homogeneous nanosized mixed nano ferrites. The FESEM images show the morphology of the prepared samples at different magnifications and have almost homogeneous. distribution, although some of them are agglomerated. The EDS data gives the elemental percent and atomic percent of the bi-doped nickel-ferrite system. And which shows the presence of Ni, Fe, O, and Bi (except x = 0) participating cations. The X-ray diffraction patterns confirm the formation of a cubic spinal structure and that the Bi ions were effectively incorporated into the NiFe2 O4 crystal lattice to form a stable Bi x Ni1-x Fe2 O4 substitution solid solution. The FT-IR spectra of the compositions under investigation reveal the formation of a single-phase cubic spinal structure. This shows two significant absorption bands, which confirm the characteristics of the ferrite sample.A

REFERENCES

A. Goldman, 2006. Modern Ferrite Technology, Springer, New York,.

Abdullah, M. Z., Al-Timimi, M. H., Albanda, W. H., Dumitru, M., Balan, A. E., Ceaus, C., ... & Stamatin, I. (2019). STRUCTURAL AND ELECTROCHEMICAL PROPERTIES OF P3-Na0. 67Mn0. 3Co0. 7O2 NANOSTRUCTURES PREPARED BY CITRIC-UREA SELF-COMBUSTION ROUTE AS CATHODE FOR SODIUM ION BATTERY. Digest Journal of Nanomaterials and BIOSTRUCTURES, 14(4), 1179-1193.

Abdullah, M. Z., Hasan, H. M., Al-Timimi, M. H., Albanda, W. H., Alhussainy, M. K., & Dumitru, M. (2019). PREPARATION AND CHARACTERIZATION

OF CARBON DOPED LITHIUM IRON PHOSPHATE COMPOSITE AS CATHODE FOR RECHARGABLE BATTERY. Journal of Ovonic Research Vol, 15(3), 199-204.

Al-Mgrs, Saad Sh Habeeb, et al. 2023"Structural and optical characterizations of synthesized CMC/PVP-SnO2 nano composites." AIP Conference Proceedings. Vol. 2475. No. 1. AIP Publishing LLC,.

Balideh, S., et al. (2021)."Structural and Magnetic Properties of Spinel Nickel-Cobalt Ferrite Nanoparticles Substituted by Dysprosium Cation Synthesized by Hydrothermal Method." Acta Physica Polonica, A. 140.1.

D. H. Chen and X. Rong He, (2001).Synthesis of nickel ferrite nanoparticles by sol-gel method, Materials Research Bulletin 36 ,1369–1377.

Kambale, R.C., Song, K.M., Koo, Y.S. and Hur, N. (2011) Low Temperature Synthesis of Nano Crystalline Dy+3 Doped Cobalt Ferrite: Structural and Magnetic Properties. Journal of Applied Physics, 110.

L. Aung, A. Khine, Kh. N. Win and M. M. Maung.2020.SYNTHESIS AND CHARACTERIZATION OF NICKEL DOPED BISMUTH FERRITE MATERIALS, J. Myanmar Acad. Arts Sci. Vol. XVIII.No.2A.

M. J. N. Isfahania, M. J. Fesharakib and V. S. 2013. Epela, Magnetic behavior of nickel–bismuth ferrite synthesized by a combined sol–gel/thermal method, Ceramics International 391163–1167.

M.Eghbali Arani, M.J. Nasr Isfahani, M.Almasi Kashi. 2010. Preparation and magnetic studies of nickel ferrite nanoparticles substituted by Sn+4 and Cu+2, Journal of Magnetism and Magnetic Materials 322,2944.

M.J. Nasr Isfahani, M. Myndyk, D. Menzel, A. Feldhoff, J. Amighian, V. Sˇ epela´ k. 2009. Magnetic properties of nanostructured MnZn ferrite, Journal of Magnetism and Magnetic Materials 321,152.

M.J. Nasr Isfahani, M. Myndyk, V. Sˇ epela´ k, J. Amighian, A Mo¨ ssbauer. 2009. effect investigation of the formation of MnZn nanoferrite phase, Journal of Alloys and Compounds 470, 434.

Maensiri, S., Masingboon, C., Boonchom, B. and Seraphin, S. (2007) A Simple Route to Synthesize Nickel Ferrite(NiFe2O4) Nanoparticles Using Egg White. Scripta Materialia, 56, 797-800.

Saeed, F. R., et al. (2017)."Nanomagnetite enhanced paraffin for thermal energy storage applications." Digest Journal of Nanomaterials and Biostructures 12.2: 273-280.

Saeed, F. R., et al. (2018). "THERMAL PROPERTIES OF PARAFFIN/NANO-MAGNETITETREVORITE PHASE CHANGE MATERIALS." Journal of Ovonic Research 14.5.

Srivastava, M., Chaubey, S. and Ojha, A.K. (2009) Investigation on Size Dependent Structural and Magnetic Behavior of Nickel Ferrite Nanoparticles Prepared by Sol-Gel and Hydrothermal Methods. Materials Chemistry and Physics118, 174-180.

Srivastava, M., Ojha, A.K., Chaubey, S., Sharma, P.K. and Pandey, A.C. (2010) Influence of pH on Structural Morphology and Magnetic Properties of Ordered Phase Cobalt Doped Lithium Ferrites Nanoparticles Synthesized by Sol- Gel Method. Materials Science and Engineering B, 175, 14-21.

V. Sˇ epela´ k, A. Feldhoff, P. Heitjans, F. Krumeich, D. Menzel, F.J. Litterst, I. Bergmann, K.D. Becker. 2006. Nonequilibrium cation distribution, canted spin arrangement, and enhanced magnetization in nanosized MgFe2O4 prepared by a one-step mechanochemical route, Chemistry of Materials 183,057.

V. Sˇ epela´ k, I. Bergmann, A. Feldhoff, P. Heitjans, F. Krumeich, D. Menzel, F.J. Litterst, S.J. Campbell, K.D. Becker, (2007). Nanocrystalline nickel ferrite, NiFe2O4: mechanosynthesis, nonequilibrium cation distribution, canted spin arrangement, and magnetic behavior, Journal of Physical Chemistry C 111 ,5026.

V. Sˇ epela´ k, K.D. Becker. (2004). Comparison of the cation inversion parameter of the nanoscale milled spinel ferrites with that of the quenched bulk materials, Materials Science and Engineering A 375–377 ,861.

Zaki, H.M. and Dawoud, H.A. (2010) Far-Infrared Spectra for Copper-Zinc Mixed Ferrites. Physica B, 405, 4476-4479.

Zhou, B., Zhang, Y.W., Liao, C.S., Yan, C.H., Chen, L.Y. and Wang, S.Y. (2004). Rare-Earth-Mediated Magnetism and Magneto-Optical Kerr Effects in Nano-Crystalline CoFeMn0.9RE0.1O4 Thin Films. Journal of Magnetism and Magnetic Materials, 280, 327-333.